Available online at www.sciencedirect.com
SCIENCE DIRECT®
Talanta 61 (2003) 643–650
Talanta
www.elsevier.com/locate/talanta

Cathodic stripping voltammetry of trace Mn(II) at carbon film electrodes

Olga M.S. Filipe [a], Christopher M.A. Brett [b,*]

[a] Escola Superior Agrária de Coimba, Bencanta, 3040-316 Coimbra, Portugal
[b] Departamento de Química, Universidade de Coimbra, 3004-535 Coimbra, Portugal

Received 29 January 2003; received in revised form 7 May 2003; accepted 21 May 2003

Abstract

A sensitive voltammetric method is presented for the determination of tract levels of Mn (II) using carbon film electrodes fabricated from carbon resistors of 2 Ω. Determination of manganese was made by square wave cathodic stripping voltammetry (CSV), with deposition of manganese as manganese dioxide. Chronoamperometric experiments were made to study MnO_2 nucleation and growth. As a result, it was found to be necessary to perform electrode conditioning at a more positive potential to initiate MnO_2 nucleation. Under optimised conditions the detection limit obtained was 4 nM and the relative standard deviation for eight measurements of 0.22 nM was 5.3%. Interferences from various metal ions on the response CSV of Mn(II) were investigated, namely Cd(II), Ni(II), Cu(II), Cr(VI), Pb(II), Zn(II) and Fe(II). Application to environmental samples was demonstrated.

Keywords: Manganese; Trace metals; Cathodic stripping voltammetry; Chronoamperometry

1. Introduction

Manganese is an essential element, which plays an important role in the activation of many enzymes involved in metabolic processes of man, animals and plants. In the natural environment manganese can occur in several oxidation states (+II, +III and +IV) and in soluble and insoluble forms [1–6]; its concentration in natural waters ranges from 0.001 to 1.0 μg ml^{-1}. The maximum allowed content in waters varies according to its proposed use: for domestic water it is 0.05 μg ml^{-1} and for irrigation water is 2.0 μg ml^{-1} [7].

Because manganese is important, highly sensitive methods are required for its determination. Various techniques have been used for the determination of trace manganese in biochemical and environmental samples, such as spectrophotometry [8] and atomic absorption spectrometry [9]. Usually such techniques need enrichment steps and, furthermore, as regards selectivity and sensitivity, often favour only one of these two aspects. For these reasons, electroanalytical techniques, stripping analysis, are the most used in trace metal determination in complex samples. These techniques have been shown to be very suitable, versatile

* Corresponding author. Tel./fax: +351-239-83-5295.
E-mail address: brett@ci.uc.pt (C.M.A. Brett).

0039-9140/03/$ - see front matter
doi:10.1016/S0039-9140(03)00327-8

and rapid for multicomponent analysis, having good selectivity and sensitivity without requiring sample pretreatment before the analytical determination.

Anodic stripping voltammetry (ASV) at a hanging mercury drop or mercury film electrode has been the most commonly used form of electrochemical stripping analysis for the determination of trace metals [10,11]. This technique has been applied to the determination of manganese in the form of Mn^{2+} e.g. [12–14]. However, ASV of manganese suffers from three problems: (i) the low solubility of manganese in mercury, (ii) the deposition potential for Mn(II) by reduction which is close to the hydrogen ion reduction potential (-1.7 V vs. SCE), and (iii) the formation of intermetallic compounds at the mercury electrode [15,16]. Consequently, there is not sufficient sensitivity in the analysis.

Adsorptive stripping voltammetry has also been used in manganese determination at both hanging mercury drop [17–21] and glassy carbon [22] electrodes. A potentiometric stripping method has also been developed and applied to waste waters [23].

Cathodic stripping voltammetry (CSV) has been less used in general, but the fact that it can be carried out without use of mercury is advantageous and with no interference from dissolved oxygen. Traces of manganese have been determined by CSV using a variety of solid electrodes (carbon, modified carbon paste, platinum, and boron doped diamond) [4,15,16,19,24–27]. The determination of manganese (II) by CSV involves a preconcentration step where the trace Mn(II) is anodically oxidised to Mn(IV) which immediately hydrolyses to form manganese dioxide (or its hydrate) on the electrode surface. The deposit of MnO_2 is then reduced to Mn(II) in the determination step.

New electrode materials have been investigated in recent years for electroanalytical applications, in many cases to avoid the use of mercury in voltammetric procedures involving reduction processes, given current legislation. These materials have included various forms of carbon. Zinc ions have been recently been measured at submicromolar concentration levels by square wave anodic stripping voltammetry following deposition at -1.55 V vs. SCE at carbon film electrodes fabricated from resistors [28]. At boron-doped diamond electrodes, lead ions have been measured by differential pulse ASV at submicromolar concentrations following deposition at -1.0 V vs. SCE [29], a mixture of zinc, lead and cadmium ions by linear sweep ASV [30] and manganese ions by ultrasound-enhanced CSV [27].

The aim of this work was to investigate the possibility of use of carbon film electrodes on a ceramic support fabricated from resistors in the determination of Mn(II) by CSV. These electrodes have a wide potential window for both positive and negative limits, exhibit good electrode kinetics for model electroactive species, are more inert than many other forms of carbon, and show attractive potentialities for application to a variety of voltammetric and electroanalytical procedures [28].

2. Experimental

2.1. Preparation of the carbon film electrode

Electrodes were made from carbon film resistors (2 Ω nominal resistance). These resistors are fabricated from ceramic cylinders of length 0.4 cm and external diameter 0.15 cm by pyrolytic deposition of carbon from methane in a nitrogen atmosphere [28]. Each resistance has two tight-fitting metal caps as external contact. To make the electrodes one of these metal caps was removed and the other was protected by normal epoxy resin. The exposed electrode geometric area was 0.2 cm^2.

The electrodes were electrochemically pretreated by cycling the electrode three times in 1 M perchloric acid solution between potential limits defined by a maximum current of ± 1 mA at a scan rate of 100 mV s^{-1} [28].

2.2. Apparatus

Voltammetric experiments were carried out using a μAutolab potentiostat (Eco Chimie, Utrecht, The Netherlands) controlled by GPES

4.5 software or with a BAS CV-50W analyser (Bioanalytical Systems) with BAS 50W 2.1 software.

Measurements were made in a glass cell containing a platinum foil auxiliary electrode and a saturated calomel electrode (SCE) as reference.

2.3. Reagents and solutions

All solutions were made from analytical grade reagents and Milli-Q ultrapure water (resistivity ≥ 18 MΩ cm). Solutions used in the influence of pH on manganese dioxide formation and reduction were 0.1 M $CH_3COOH/NaCH_3COO$ buffer, 0.2 M NaH_2PO_4/Na_2HPO_4 buffer, and 0.2 M H_3BO_3 in 0.1 M KCl, adjusting the pH with 1.0 M NaOH. Manganese ion standard solutions were prepared by diluting a 10^{-3} M Mn^{2+} solution, prepared from manganese sulphate, in the chosen supporting buffer electrolyte. Experiments were carried out at 24 ± 1 °C without the removal of oxygen.

Porewater samples from a stream near a disused mine in southern Portugal were extracted by squeezing a composite sediment sample against a 10 μm Teflon mesh with pure nitrogen at 2 atm, pH 7.1. Samples were preserved by acidification to pH 2 with nitric acid, according to the procedure in Ref. [31], stored frozen, and after unfreezing diluted in pH 7.2 buffer electrolyte immediately before analysis.

2.4. Procedure

In CSV experiments, the metal ions were preconcentrated directly on the 2 Ω carbon film surface by electrodeposition and then stripped by a negative square-wave voltammetric potential scan. After optimisation to be described below, the deposition was carried out at 0.8 V vs. SCE during 120 s after electrode conditioning at 1.0 V vs. SCE during 10 s; the square wave (sw) parameters were: frequency 25 Hz, scan increment 4 mV, amplitude 20 mV.

3. Results and discussion

The influence of solution pH on the oxidation of Mn(II) at the carbon film electrode and its subsequent reduction as well as the process of formation of MnO_2 were investigated. SWCSV parameters were optimised and analyses performed, together with a study of possible interferences from other metal ions.

3.1. Effect of pH

The oxidation process of manganese is dependent on pH. Eq. (1) describes the chemical reaction that occurs, assuming stoichiometric formation of MnO_2, as previously shown [15]:

$$Mn^{2+} \rightarrow MnO_2 + 4H^+ + 2e^- \quad (1)$$

Fig. 1 shows the influence of the pH on the redox process of manganese in different supporting electrolytes, as measured by cyclic voltammetry. The potentials of the anodic peak and of the cathodic peak shift towards more negative values with increasing pH. By plotting E vs. pH, the predicted slope is 118.25 mV, corresponding to a four proton and two electron process. An experimental value of 133 and 130 mV, for pH values between 4.5 and 9.0, was obtained for anodic and

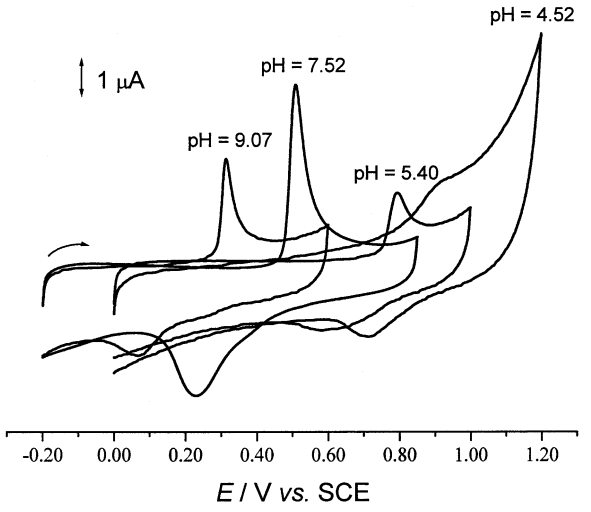

Fig. 1. Cyclic voltammograms of 1.04×10^{-5} M Mn^{2+} at carbon film electrode in different supporting electrolytes at various pH values. Scan rate 100 mV s^{-1}.

cathodic peaks respectively. The shape and position of the anodic peaks suggests that the oxidation reaction is diffusion-controlled.

Outside this range of pH lower oxidation and reduction peak heights were observed. At low pH (<4) [15,32], there is a tendency for incomplete precipitation of the insoluble dioxide, which leads to a lower peak height. However, at higher pH (>12), the decrease in the peak height can be attributed to the increasingly competitive production of $Mn(OH)_2$, which can react with dissolved oxygen to precipitate $Mn(OH)_4$ in solution. The extent to which this will affect the electrode reaction depends on the solubility product, K_s, $(Mn(OH)_2) = 2 \times 10^{-13}$ [15]. Consequently, the use of an electrolyte in neutral or slightly acid solution is suggested.

Thus, pH 7.2 was chosen with 0.2 M H_3BO_3/0.1 M KCl as supporting electrolyte because a very well defined reduction peak was obtained (see Fig. 1); this electrolyte had previously been used successfully in Mn(II) redox process studies [15,32,33].

3.2. SWCSV deposition potential

Illustrative stripping voltammograms obtained from measurements of manganese (II) at several different deposition potentials are shown in Fig. 2. It can be seen that the peak current decreases when the deposition potential is changed to more positive values. A deposition potential of 0.8 V was chosen. Less positive values also led to decreased stripping currents.

3.3. Square wave parameters

The square wave frequency, amplitude and potential increment were all optimised. There was very little effect of the square wave amplitude over the range 10–30 mV and of the square wave potential increment over the range 2–4 mV. The values chosen were 20 and 4 mV, respectively. Over the square wave frequency range 5–50 Hz, the stripping peak current increases; the frequency chosen was 25 Hz.

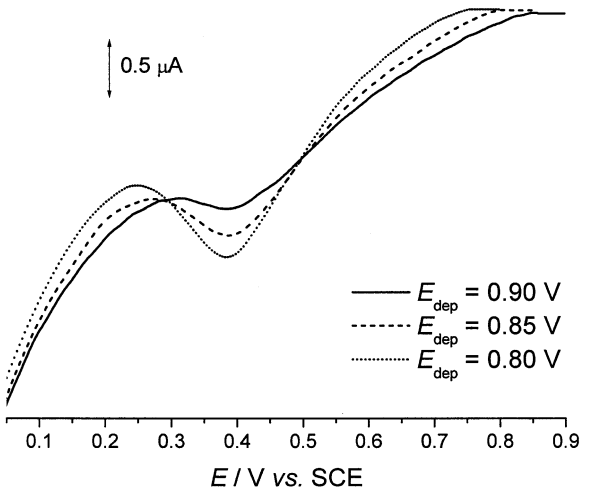

Fig. 2. Effect of deposition potential on peak current. $[Mn^{2+}] = 0.101$ μM in 0.2 M H_3BO_3/0.1 M KCl pH 7.2; $f =$ 25 Hz, amp = 20 mV, $\Delta E = 4$ mV and $t_{dep} = 120$ s with stirring.

3.4. Nucleation process of MnO_2

When the effect of the concentration of Mn^{2+} was studied using the experimental parameters optimised above together with a deposition potential of 0.8 V and 120 s deposition, a linear relationship between the concentration and peak current was observed, but with a very negative intercept. This suggests the existence of an induction time for deposition, which could be due to a slow MnO_2 nucleation process.

For investigating the MnO_2 nucleation process and growth some chronoamperometric experiments were carried out with different Mn^{2+} concentrations in the range 10^{-8} to 10^{-5} M and by applying a potential step from 0.5 V (before any MnO_2 deposition under these conditions) to different more positive potential values.

In nucleation processes the current observed is a function of t^n, where n depends on the type of nucleation involved, the growth phase geometry and on the rate-determining step in the nucleation step. Various growth models for anodic oxide films and characteristics are summarized in Ref. [34]. With respect to the dependence of the chronoamperometric current dependence on t, they are:

$t^{-1/2}$ formation of a homogeneous oxide layer

t^0 formation of an unstable layer
instantaneous 1D nucleation

t^1 instantaneous 2D nucleation
progressive 1D nucleation

t^2 progressive 2D nucleation

Fig. 3 is a plot of slope values from the log I vs. log t plots vs. potential for various Mn^{2+} solutions in the concentration range 10^{-8} to 10^{-3} M in H_3BO_3/KCl at pH 7.2. The slope, n, of the plots varies between ≈ -0.5 and ≈ -0.23. This can indicate that MnO_2 formation is a mixture of between a homogenous film ($I \propto t^{-1/2}$), and normal growth through instantaneous nucleation and an unstable layer ($I \propto t^0$). At 0.8 V the slope is ≈ -0.5 for all Mn^{2+} concentrations tested suggesting formation of a homogeneous film. However, at higher potentials, although more oxide is deposited, the film is less homogeneous and potentially unstable. This agrees with the results illustrated in Fig. 2, where at more positive deposition potentials the reduction current becomes less.

These results are in agreement with the previously proposed multistep MnO_2 deposition mechanisms [35–37]. Rodrigues et al. [35] suggest that the oxidation of Mn^{2+} ions to MnO_2 follows the mechanism:

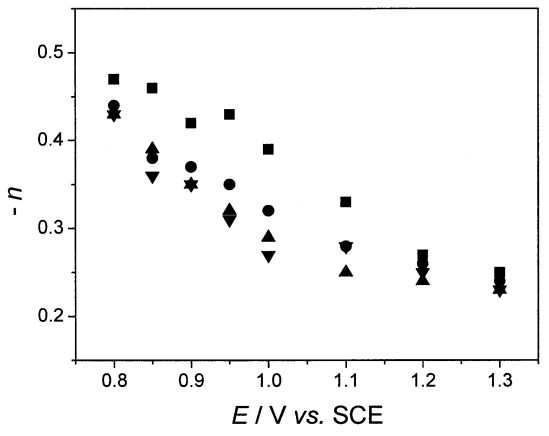

Fig. 3. Plot of slope, $-n$, vs. E_f in plots of 1 gI vs. 1 gt from chronoamperometric transients, after stepping potential from +0.5 V vs. SCE to E_f. Mn^{2+} solutions: (●) 2.03×10^{-8} M, (▲) 1.01×10^{-7} M, (▼) 2.32×10^{-6} M and (■) 1.04×10^{-5} M in pH 7.2 0.2 M H_3BO_3/0.1 M KCl electrolyte.

Step 1: $Mn^{2+}_{(solution)} \rightarrow Mn^{2+}_{(surface)}$
Step 2: $Mn^{2+}_{(surface)} \rightarrow Mn^{3+}_{(adsorbed)} + e^-$
Step 3: $H_2O \rightarrow OH_{(adsorbed)} + H^+ + e^-$
Step 4: $2Mn^{3+}_{(adsorbed)} \rightarrow Mn^{2+}_{(adsorbed)} + Mn^{4+}_{(adsorbed)}$
Step 5: $Mn^{2+}_{(adsorbed)} + 2OH_{(adsorbed)} \rightarrow MnO_2 + 2H^+$
Step 6: $Mn^{4+}_{(adsorbed)} + 2H_2O \rightarrow MnO_2 + 4H^+$

Nijjer et al. [36] suggested that oxidation of Mn^{2+} to MnO_2 occurs by an ECE mechanism, the chemical reaction of Mn^{3+} to form MnOOH being the rate determining step:

Step 4a: $Mn^{3+}_{(adsorbed)} + 2H_2O \rightarrow MnOOH_{(adsorbed)} + 3H^+$
Step 5a: $MnOOH_{(adsorbed)} \rightarrow MnO_2 + H^+ + e^-$

also considered by Kao and Weibel [37]. According to Ref. [36], nucleation of MnO_2 is dominated by an equilibrium involving a Mn(III) intermediate, steps 4 and 4a. Subsequent growth of MnO_2 involves the reduction of MnO_2 surfaces by Mn^{2+} ions in solution to form MnOOH and/or Mn^{3+} intermediate depending on the local pH and potential:

$$Mn^{2+} + MnO_2 + H^+ \rightarrow MnOOH + Mn^{3+}$$

$$Mn^{2+} + MnO_2 + 2H_2O \rightarrow 2MnOOH + 2H^+$$

This means that at low Mn^{2+} concentration, diffusion of Mn^{2+} ions from bulk solution to the MnO_2/electrolyte interface is a factor controlling the growth of MnO_2 and it follows a CE mechanism, in which the chemical step is rate-determining.

The reverse process on scanning the potential in a negative direction is

$$MnO_2 + H^+ + e^- \rightarrow MnOOH$$

$$MnOOH + 3H^+ + e^- \rightarrow Mn^{2+} + 2H_2O$$

assuming perfect stoichiometry of the manganese dioxide. In fact there are several different crystalline forms of MnO_2 which could influence the ease

of reductive dissolution [38]. There is also the possibility of some cation incorporation, such as interstitial K^+ together with Mn(III) in the MnO_2 structure during manganese dioxide growth [39,40], which would reduce the charge observed during the reduction process. These questions have been extensively studied for manganese dioxide formed on different electrode substrates [38,41–43].

From the chronoamperometric results it was concluded that it was necessary to perform electrode preconditioning at a more positive potential to initiate MnO_2 nucleation, at a value between 1.0 and 1.3 V, for the Mn^{2+} concentrations 10^{-8} to 10^{-7} M. If it is considered that the MnO_2 nucleation process involves a Mn(III) intermediate, as discussed above, then these potential values are acceptable. At a high positive potential more Mn^{3+} ions are produced and the equilibria of steps 4 and 4a are forced to the right to form MnO_2 (steps 5, 5a and 6), which initiate growth. To avoid the problem of unstable layer formation, the potential applied should be made less positive once the nuclei have been formed.

Two different potential values (1.0 and 1.3 V) and two different times (3 and 10 s), for different Mn^{2+} concentrations were chosen to observe the influence of these parameters experimentally on SWCSV; the results are shown in Fig. 4. At 1.0 V preconditioning potential the peak current is higher than without preconditioning, and the intercept is closer to zero.

Applying more positive preconditioning potentials than 1.0 V causes a decrease of the peak current, probably due to flaking off of unstable nuclei. There is no significant difference between preconditioning times of 3 and 10 s.

Thus, a preconditioning potential of 1.0 V during 10 s to favour MnO_2 nucleation was used in further experiments.

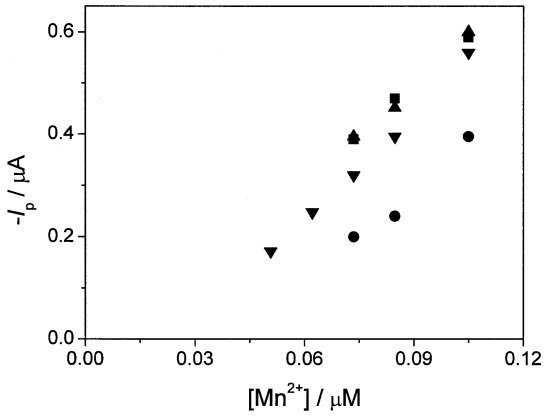

Fig. 4. Plot of SWCSV peak current vs. Mn^{2+} concentration for different preconditioning potentials, E_{con} and times, t_{con}. $t_{dep} = 120$ s with stirring and $E_{dep} = 0.8$ V; (▼) without preconditioning, (■) $E_{con} = 1.0$ V and $t_{con} = 3$ s, (▲) $E_{con} = 1.0$ V and $t_{con} = 10$ s, (●) $E_{con} = 1.3$ V and $t_{con} = 10$ s. SW parameters: $f = 25$ Hz, amp = 20 mV, $\Delta E = 4$ mV.

3.5. Calibration plot and precision

The SWCSV response for successive standard additions of manganese ion was studied in 0.2 M H_3BO_3/0.1 KCl solution at pH 7.2. The electrode was preconditioned at 1.0 V during 10 s with stirring and the deposition potential was 0.8 V during 180 s with stirring. Linear relations between peak current and Mn^{2+} concentration in two different regions were observed, as shown in Fig. 5. The two regions could be due to the formation of mono and multilayers of MnO_2, although different forms of MnO_2 with some incorporated potassium ions could also play a role (see Section 3.4). Least-squares treatment of the first linear region yielded a slope of 3.913 ± 0.282 A/M, an

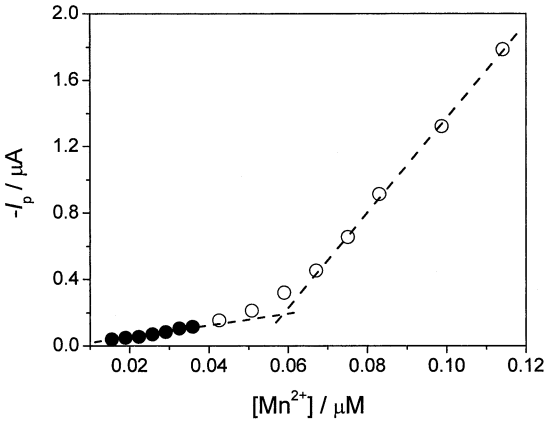

Fig. 5. Plot of I_p vs. $[Mn^{2+}]$ for SWCSV of Mn^{2+} in 0.2 M H_3BO_3/0.1 M KCl pH 7.2 electrolyte. $E_{con} = 1.0$ V, $t_{con} = 10$ s, $E_{dep} = 0.8$ V, $t_{dep} = 180$ s with stirring. SW parameters: $f = 25$ Hz, amp = 20 mV, $\Delta E = 4$ mV.

intercept of -0.027 ± 0.008 μA and a correlation coefficient of 0.988 ($N = 7$). The detection limit calculated by the method described in Ref. [44] was 3.9 nM. The detection limit obtained is of the same order of magnitude as obtained by other authors using CSV at solid electrodes [4,16,24,25].

Concerning reproducibility, the peak current from eight consecutive measurements of a 22.4 nM Mn^{2+} solution had a relative standard deviation (R.S.D.) of 5.3%, and the R.S.D. of the calibration slope obtained on three different days and carbon film electrodes was 10.8%. We can conclude that carbon film electrodes have good reproducibility. However, if the electrode is used for more than two complete analytical calibration curves, although a small progressive increase of sensitivity is observed the reproducibility is less, which can reflect modifications of the surface state.

3.6. Interferences

Interferences from a number of metal ions: Cd(II), Ni(II), Cu(II), Cr(VI), Pb(II), Zn(II) and Fe(II) on the CSV of 60 nM Mn(II) were investigated. The criterion used for an interference was a peak height varying by more than 5% from the expected value. The results obtained are shown in Table 1. The main deductions from the results obtained are:

(i) Cd(II), Cr(VI) and Zn(II) do not interfere in the MnO_2 signal even when present in a 109-fold excess.

(ii) Ni(II) and Cu(II) lower the peak height about 60% if the concentration is 109 fold excess, and copper interference at a similar level is caused by the reduction peak of Cu^{2+} at -0.040 V vs. SCE masking the MnO_2 peak.

(iii) The presence of Pb(II) in solution in concentrations equal to that of manganese does not interfere. However, an increase in the Pb/Mn ratio leads to a larger and higher peak, and the potential moves to more negative values, which agrees with the observation of Jin et al. [16]. This interference is probably due to the fact that Pb(II) is easily oxidized to PbO_2 which can be co-deposited onto the electrode surface together with manganese oxide.

Table 1
Influence of other metal ions on the manganese stripping peak (60 nM Mn^{2+})

Metal ion	Metal/manganese molar ratio	ΔI_p (%)
Cd^{2+}	109	$< +3$
Zn^{2+}	109	$< +4$
CrO_4^{2-}	109	$< +4$
Ni^{2+}	1	+5
	10	−14
	50	−44
	109	−57
Cu^{2+}	1	−8
	10	−37
	49	−50
	108	−59
Pb^{2+}	1	5
	10	31
	49	50
Fe^{2+}	1	−12
	10	−59
	49	−55
	109	−100

(iv) The presence of Fe(II) in equimolar amounts affects the determination of manganese ions as also observed by Saterlay et al. [27].

3.7. Application to real samples

Application to environmental samples was tested with porewater from sediment samples from a stream next to a disused mine in southern Portugal, see Section 2 for details of preparation. These contain a number of metal ions in a complex matrix and concentrations were determined using a 5-point standard addition method. The samples had to be diluted a factor of 1000 in buffer electrolyte to ensure that they lay within the first linear region of the calibration curve (Fig. 5). The results obtained were: 10.2 ± 1.0 μM immediately after sample unfreezing and 12.3 ± 0.8 μM after 1 week which demonstrated good agreement compared with independent analysis by ICP-AAS. The reason for the change in concentration can be attributed to the slow dissolution, and thence increase in chemically labile fraction, of manganese in insoluble forms on microscopic particles in suspension in the samples.

4. Conclusions

The results of this work show that carbon film electrodes fabricated from 2 Ω carbon resistors can be successfully applied to the electroanalysis of traces of manganese ions by CSV and demonstrate yet another use for these cheap and robust electrode materials. Under optimised conditions, a detection limit of 4 nM was obtained. Nucleation and growth of manganese dioxide on the carbon surface was investigated, leading to optimisation of the potential scheme in the preconcentration step. Application to environmental samples has been demonstrated.

Acknowledgements

The financial support of ICEMS, Coimbra (Research Unit 103) is gratefully acknowledged. The authors thank Dr Rui Ribeiro, Instituto do Ambiente e Vida, Coimbra, Portugal for the samples of porewater.

References

[1] T.M. Florence, Talanta 29 (1982) 345.
[2] T.M. Florence, Analyst 111 (1986) 489.
[3] T.M. Florence, G.E. Batley, CRC Crit. Rev. Anal. Chem. 9 (1980) 219.
[4] J. Labuda, M. Vanicková, E. Beinrohr, Mikrochim. Acta I (1989) 113.
[5] B. Chiswell, M.B. Mokhtar, Talanta 33 (1986) 669.
[6] G. Davies, Coordin. Chem. Rev. 4 (1969) 199.
[7] M.P. Colombini, R. Fuoco, Talanta 30 (1983) 901.
[8] N. Maniasso, E.A.G. Zagatto, Anal. Chim. Acta 366 (1998) 87.
[9] C. Sarznini, O. Abollino, E. Mentasti, Anal. Chim. Acta 435 (2001) 343.
[10] C.M.G. van den Berg, Anal. Chim. Acta 250 (1991) 265.
[11] Kh.Z. Brainina, N.A. Malakhova, N.Yu. Stojko, Fresenius. J. Anal. Chem. 368 (2000) 307.
[12] R.J. O'Halloran, Anal. Chim. Acta 140 (1982) 51.
[13] M.M. Ghoneim, A.M. Hassanein, E. Hammam, A.M. Beltagi, Fresenius. J. Anal. Chem. 367 (2000) 378.
[14] C. Locatelli, G. Torsi, J. Electroanal. Chem. 509 (2001) 80.
[15] C.M.A. Brett, M.M.P.M. Neto, J. Electroanal. Chem. 258 (1989) 345.
[16] J.-Y. Jin, F. Xu, T. Miwa, Electroanalysis 12 (2000) 610.
[17] J. Wang, J.S. Mahmoud, Anal. Chim. Acta 182 (1986) 147.
[18] A. Romanus, H. Muller, D. Kirsch, Fresenius. J. Anal. Chem. 340 (1991) 363.
[19] L. Wang, C. Ma, X. Zhang, J. Wang, Anal. Lett. 26 (1993) 171.
[20] J. Wang, J. Lu, Talanta 42 (1995) 331.
[21] O. Abollino, M. Aceto, C. Sarzanini, E. Mentasti, Electroanalysis 11 (1999) 870.
[22] N.A. El-Maali, D.A. El-Hady, Anal. Chim. Acta 370 (1998) 239.
[23] G.R. Scollary, G.N. Chen, T.J. Cardwell, V.A. Vincente-Beckett, Electroanalysis 7 (1995) 386.
[24] I. Vos, Z. Komy, G. Reggers, E. Roekens, R. Van Grieken, Anal. Chim. Acta 184 (1986) 271.
[25] J.S. Roitz, K.W. Bruland, Anal. Chim. Acta 344 (1997) 175.
[26] S.B. Khoo, M.K. Soh, Q. Cai, M.R. Khan, S.X. Guo, Electroanalysis 9 (1997) 45.
[27] A.J. Saterlay, J.S. Foord, R.G. Compton, Analyst 124 (1999) 1791.
[28] C.M.A. Brett, L. Angnes, H. Liess, Electroanalysis 13 (2001) 765.
[29] A. Manivannan, D.A. Tryk, A. Fujishima, Electrochem. Solid State Lett. 2 (1999) 455.
[30] M.C. Granger, J. Xu, J.W. Stojek, G.M. Swain, Anal. Chim. Acta 397 (1999) 145.
[31] A.D. Eaton, L.S. Clesceri, A.E. Greenberg (Eds.), Standard Methods for the Examination of Water and Wastewater, American Public Health Association, Washington DC, 1995.
[32] E. Hrabankova, J. Dolezal, V. Masin, J. Electroanal. Chem. 22 (1969) 195.
[33] E. Kostihova, P. Beran, Coll. Czech. Chem. Commun. 47 (1982) 1216.
[34] J.W. Schultze, M.M. Lohrengel, Electrochim. Acta 28 (1983) 973.
[35] S. Rodrigues, N. Munichandraiah, A.K. Shukla, J. Appl. Electrochem. 28 (1998) 1235.
[36] S. Nijjer, J. Thonstad, G.M. Haarberg, Electrochim. Acta 46 (2000) 395.
[37] W.H. Kao, V.J. Weibel, J. Appl. Electrochem. 22 (1992) 21.
[38] S. Bakardjieva, P. Bezdicka, T. Grygar, P. Vorm, J. Solid State Electrochem. 4 (2000) 306.
[39] P. Ruetschi, R. Giovanoli, J. Electrochem. Soc. 135 (1988) 2663.
[40] W.H. Kao, V.J. Weibel, M.J. Root, J. Electrochem. Soc. 139 (1992) 1223.
[41] S. Bodoardo, J. Brenet, M. Maja, P. Spinelli, Electrochim. Acta 39 (1994) 1999.
[42] J.M. Amarilla, F. Tedjar, C. Poinsignon, Electrochim. Acta 39 (1994) 2321.
[43] B.L. Wu, D. Lincot, J. Vedel, L.T. Yu, J. Electroanal. Chem. 420 (1997) 159.
[44] J.N. Miller, J.C. Miller (Eds.), Statistics and Chemometrics for Analytical Chemistry, fourth ed. (Chapter 5), Prentice Hall, NJ, 2000 (Chapter 5).